Boundary layer analysis and heat transfer of a nanofluid

M.M. MacDevette, T.G. Myers, B. Wetton

BOUNDARY LAYER ANALYSIS AND HEAT TRANSFER OF A NANOFLUID

M.M. MACDEVETTE, T.G. MYERS, B. WETTON

ABSTRACT. A theoretical model for nanofluid flow, including Brownian motion and thermophoresis, is developed and analysed. Standard boundary layer theory is used to evaluate the heat transfer coefficient near a flat surface. The model is almost identical to previous models for nanofluid flow which have predicted an increase in the heat transfer with increasing particle concentration. In contrast our work shows a marked decrease indicating that under the assumptions of the model (and similar ones) nanofluids do not enhance heat transfer. It is proposed that the discrepancy between our results and previous ones is due to a loose definition of the heat transfer coefficient and various *ad hoc* assumptions.

1. INTRODUCTION

There exists a vast literature regarding the behaviour and applications of nanofluids. In particular the often remarkable experimental results concerning their heat transfer properties has seen them proposed as a front runner in the race to cool modern high performance electronic equipment. However, there appears no real consensus on whether nanofluids are indeed capable of removing large amounts of heat. The plethora of experimental papers promoting their efficiency and enhanced thermal conductivity, see [15, 16, 20] for example, appeared to have been superseded by the benchmark study [6] carried out in over 30 organisations throughout the world which suggested no anomalous enhancement of thermal conductivity in the fluids tested. Indeed this should not be too surprising since heat conduction occurs due to the transfer of kinetic energy from hot, rapidly vibrating atoms or molecules to their cooler, more slowly vibrating neighbours. In solids the close, fixed arrangement of atoms means that conduction is more efficient than in fluids, which have a larger distance between atoms [30]. A nanofluid is made up of a small quantity of solid particles separated by a large amount of fluid, thus ruling out the possibility of a great deal of intimate contact between particles and hence suggesting no significant increase in thermal conductivity. This conclusion is backed up by a small number of other theoretical and experimental papers showing a degradation in thermal performance with increasing volume fraction [15, 32, 40]. Yet despite this conclusion nanofluids and their heat

transfer properties are still the subject of numerous articles, as discussed in the recent review [20].

In addition to the lack of consensus on physical properties there is not yet an accepted model for nanofluid flow. A number of models and physical mechanisms (which may or may not be important) are described in [10]. In this paper we will focus on a particular form of model, originally proposed by Buongiorno [5], which includes thermophoresis and Brownian motion. In [5] an order of magnitude study was carried out to dismiss a number of heat transfer mechanisms and show that thermophoresis and Brownian motion play a significant role in the energy transport of a flowing liquid. He then analysed a boundary layer flow model to demonstrate an increase in heat transfer coefficient with particle volume fraction. Subsequently various theoretical papers based on the same model have verified this conclusion [17, 23, 25, 39]. Evans *et al.* [14] concluded that Brownian motion has a negligible effect on the thermal conductivity. Savino and Paterna [34] study buoyancy driven flow in a 1mm wide channel, they conclude that Brownian motion and thermophoresis do affect the flow, but only over a time-scale of 27 hours, with the results most noticeable when gravity is 10^{-6} of its normal value. The real goal in the development of nanofluids for cooling purposes is to enhance the heat transfer and energy removal from a given surface. To understand this requires knowledge of the flow and heat transfer coefficient (HTC) at the interface between the fluid and the solid. This is the aim of the present paper. The HTC is a surprisingly poorly defined quantity so, in the following section, we will begin by examining the HTC and defining it in a way that reflects the correct heat transfer from a surface. We will then develop a similar model to that of [5, 34] via the energy and momentum equations defined in *et al.* [4, Ch. 3]. Standard boundary layer scaling will be applied to reduce the equations and, in particular, demonstrate that Brownian motion and thermophoresis are negligible with the boundary layer. We go on to show that, for the fluid-particle systems investigated, *the HTC decreases with increasing particle volume fraction*. Finally, given the number of papers that have reached the opposite solution from the same equations we briefly discuss reasons for this discrepancy. Throughout the paper we will work with a water-based nanofluid, although parameter values and some results are also reported for Ethyene Glycol based nanofluids.

2. Calculating the heat transfer coefficient

The goal of this paper is to determine whether the addition of nanoparticles to a base fluid can improve its ability to transfer heat. It is important to bear in mind that this heat transfer depends not only on the heat removal from the surface but also how well the fluid transports the energy away. For example, although the nanofluid may have a higher heat capacity than the base fluid, this increased ability to store thermal energy may be offset by the increase in fluid viscosity, meaning energy transport with the flow is slower. Hence, in assessing the fluid's

heat removal ability we must consider the coupled problem of heat and fluid flow. A second significant issue in analysing the heat removal is the concept of the heat transfer coefficient. This is the parameter used by many authors to quantify the heat transfer from a solid to a fluid. However, it is loosely defined and often does not truly reflect the amount of heat transferred to the fluid. Consequently, before we move on to the full thermal model we will begin with a discussion of the HTC.

When fluid flows over a solid surface the HTC represents the ratio of heat input at the boundary to that transferred to the fluid. If q is the energy input at the boundary per unit area and ΔT some temperature change in the fluid then the HTC is typically defined by $h = q/\Delta T$. If the no-slip condition holds at the solid-liquid boundary then the heat transfer there is by conduction, rather than convection, and so Fourier's law holds,

$$(1) \qquad\qquad q = -k \left.\frac{\partial T}{\partial y}\right|_{y=0} ,$$

where $y = 0$ denotes the position of the interface. Substituting for q leads to the standard boundary condition

$$(2) \qquad\qquad -k \left.\frac{\partial T}{\partial y}\right|_{y=0} = h\Delta T .$$

The variation in interpretation of this boundary condition comes through the choice of ΔT. Perhaps the most common choice is $\Delta T = T_w - T_\infty$, where T_w is the temperature of the solid and T_∞ that of the fluid in the far field [3, 10]. If the solid is heating the fluid, then it is well-known that $T_w > T_{y=0^+}$ and so, since $h \propto 1/\Delta T$, the definition $\Delta T = T_w - T_\infty$ will underestimate the HTC. The mathematical literature tends to favour the choice $\Delta T = T_{y=0^+} - T_\infty$, which should be closer to representing the heat passed to the fluid. In fact the two choices are often combined by choosing a mathematical description where the fluid temperature $T_{y=0^+} = T_w$. In the nanofluid literature such choices may be found in [5, 11, 32, 38] for example and there are also numerous examples in the general heat transfer literature [4].

In fact, neither of the above options actually represents the energy increase in the fluid. The problem being that the choice of ΔT is arbitrary and implicitly assumes that the temperature (or energy) rise is linear in the fluid. To correctly determine the energy rise requires knowledge of the velocity and temperature profiles in the liquid. Say a fluid enters a system at $x = 0$ with some initial temperature T_∞ and a corresponding energy flux then a distance L downstream the energy flux above the initial value is given by

$$(3) \qquad\qquad Q = \int_0^{\delta_T(L)} \rho c u (T - T_\infty)\, dy ,$$

where $\delta_T(L)$ is the thickness of the thermal boundary layer at $x = L$. In order to write a HTC in a manner similar to previous definitions we may define an

average temperature rise in the fluid T_{av} by

$$(4) \qquad (T_{av} - T_\infty) \int_0^{\delta_T} \rho c u \, dy = \int_0^{\delta_T} \rho c u (T - T_\infty) \, dy \ .$$

Note, T_{av} is referred to in [4] as the 'cup' average . The term cup average indicates that if the flow to the edge of the boundary layer at $x = L$ was collected in a cup the temperature of this fluid would be given by T_{av}. The HTC that correctly reflects the ratio of energy entering at the boundary to that transferred into the fluid is

$$(5) \qquad h = \frac{q}{T_{av} - T_\infty} = \frac{q \int_0^{\delta_T} \rho c u \, dy}{\int_0^{\delta_T} \rho c u (T - T_\infty) \, dy} \ .$$

This is the definition we will use in the following work. Note, the HTC varies with distance downstream (we have omitted writing $x = L$ in all the integrals) but will tend to an asymptote far downstream. A more detailed description of the HTC and different ways to estimate it are given in [4].

3. Mathematical Modelling

Initially we will assume fluid properties, such as density, viscosity, thermal conductivity and heat capacity, depend on the volume fraction ϕ. Hence we write down a general model to account for this. The equations governing the flow of a compressible nanofluid may be written as

$$(6) \qquad \frac{\partial \rho_{nf}}{\partial t} + \nabla \cdot (\rho_{nf} \mathbf{u}) = 0,$$

$$(7) \qquad \rho_{nf} \left[\frac{\partial \mathbf{u}}{\partial t} + \mathbf{u} \cdot \nabla \mathbf{u} \right] = -\nabla p - \nabla \cdot \tilde{\tau} + \rho_{nf} \mathbf{g},$$

$$(8) \qquad \frac{\partial(\chi_{nf} T)}{\partial t} + \nabla \cdot (\chi_{nf} \mathbf{u} T) = \nabla \cdot (k_{nf} \nabla T) + \mu_{nf} \Phi,$$

$$(9) \qquad \frac{\partial(\rho_{nf} f)}{\partial t} + \nabla \cdot (\rho_{nf} f \mathbf{u}) = \nabla \cdot \left[\rho_{nf} D_B \nabla f + \rho_{nf} D_T \frac{\nabla T}{T} \right],$$

where $\mathbf{u}$ is the velocity vector, T the temperature and g gravity. Subscripts bf, nf and np refer to the base fluid, nanofluid and nanoparticle, respectively. The density and volumetric heat capacity are defined as

$$(10) \qquad \rho_{nf} = \phi \rho_{np} + (1 - \phi) \rho_{bf},$$
$$(11) \qquad \chi_{nf} = (\rho c)_{nf} = \phi \rho_{np} c_{np} + (1 - \phi) \rho_{bf} c_{bf} \ .$$

The variable f is the mass fraction of suspended nanoparticles and related to the volume fraction by

$$(12) \qquad f = \frac{\phi \rho_{np}}{(1 - \phi) \rho_{bf}} \ ,$$

and the viscous dissipation is written as

$$(13) \qquad \Phi = \frac{\partial u_i}{\partial x_j} \left(\frac{\partial u_i}{\partial x_j} + \frac{\partial u_j}{\partial x_i} \right).$$

The derivation of equations (6–8) follows along the lines described in Bird *et al.* [4, Ch.3]. Although it should be noted that in the derivation of [4] the specific heat capacity is assumed constant. In that case combining the energy and continuity equations permits χ to be moved outside the derivative terms on the left hand side of (8). However, since the specific heat of a nanofluid is a function of ϕ for the moment we leave the equations in a slightly more general form.

Brownian diffusion is represented by the term involving D_B in equation (9), the D_T term describes thermophoresis. The velocity induced by a temperature gradient is typically written as

$$(14) \qquad v = -\beta \mu_{bf} \nabla T / (\rho_{bf} T),$$

where $\beta = 0.26 \cdot k_{bf} / (2k_{bf} + k_{np})$ is a proportionality factor between that of the slip velocity due to thermophoresis and the temperature factor $\nabla T / T$, see [2, 7, 13, 26, 34]. The thermophoretic mass flux is then $j_T = \rho_{np} \phi v$. This is often written as $j_T = -\rho_{np} \tilde{D}_T \nabla T$ where $\tilde{D}_T = \beta \mu_{bf} \phi / (\rho_{bf} T)$ is termed the thermal diffusion coefficient. However, this 'diffusion coefficient' has dimensions $m^2/(s \; K)$. Consequently in equation (9) we follow the convention of [5] in defining a dimensionally correct diffusion coefficient, $D_T = \beta \mu_{bf} \phi / \rho_{bf}$, which then requires an additional factor $1/T$ in the final term of equation (9). Vigolo *et al.* [36] also point out this discrepancy in definition and term $\tilde{D}_T$ as used by many previous authors as a *thermophoretic mobility* rather than a diffusion coefficient. The two diffusion coefficients, D_B, D_T, involve the variable temperature and mass fraction respectively,

$$(15) \qquad D_B = \frac{k_B T}{3\pi \mu_{bf} d_p}, \qquad\qquad D_T = \frac{\beta \mu_{bf} f}{\rho_{bf}},$$

where k_B is the Boltzmann constant and d_p the particle diameter. Previous studies have evaluated D_B, D_T using some reference temperature and volume fraction, whilst allowing T, ϕ to vary everywhere else in the equations, see for example [5, 34]. To clarify the dependence on temperature and volume fraction in all subsequent equations we will use constants that do not involve T, ϕ, i.e. $C_B = \frac{D_B}{T}, C_T = \frac{D_T}{f}$. Note, we write C's instead of D's to clarify that these are not the standard diffusion coefficients (and indeed C_B no longer has the correct dimensions for this).

The components of the stress tensor are given in various co-ordinate systems in [4, Ch. 3]. In Cartesian co-ordinates

$$\tilde{\tau}_{xx} = \mu_{nf} \left[-2\frac{\partial u}{\partial x} + \frac{2}{3}\nabla \cdot \mathbf{u} \right], \qquad \tilde{\tau}_{xy} = \tilde{\tau}_{xy} = -\mu_{nf} \left(\frac{\partial u}{\partial y} + \frac{\partial v}{\partial x} \right),$$

$$(16) \qquad \tilde{\tau}_{xz} = \tilde{\tau}_{xz} = -\mu_{nf}\left(\frac{\partial u}{\partial z} + \frac{\partial v}{\partial y}\right),$$

and the components $\tilde{\tau}_{yy}, \tilde{\tau}_{zz}$ follow the pattern of $\tilde{\tau}_{xx}$. The viscosity, μ_{nf}, may vary considerably with the particle volume fraction. The Brinkman relation for the viscosity significantly under predicts the true value for $\phi > 0.01$. Khanafer and Vafai [19] present a complex polynomial representation for $\mu_{nf} = \mu_{nf}(\phi, T)$ and show good agreement with data. The experiments of Prasher *et al.* [33] indicate only a weak dependence of viscosity on T and particle diameter. Corcione [9] shows a weak dependence on T but presents evidence for the diameter dependence. In the absence of agreement we will begin with a simple representation, where $\mu_{nf} = \mu_{nf}(\phi)$, given by Maiga *et al.* [25] who fitted the experimental data of a water based nanofluid by Wang *et al.* [37] with the following relation

$$(17) \qquad \mu_{nf} = (1 + 7.3\phi + 123\phi^2)\mu_{bf},$$

and for ethylene glycol based fluids,

$$(18) \qquad \mu_{nf} = (1 - 0.19\phi + 306\phi^2)\mu_{bf}.$$

The thermal conductivity of a nanofluid is a thorny issue, with much discrepancy and debate concerning the often remarkable experimental results. The basic theoretical model, the Maxwell model, provides a simple relation for k_{nf} in terms of ϕ and k_{bf}. For $\phi \ll 1$ this relation may be linearised to show

$$(19) \qquad k_{nf} = k_{bf}(1 + C_k\phi),$$

where $C_k \approx 3$. This is well-known to significantly underpredict the thermal conductivity. The Maxwell model is based on a steady-state analysis: a recent theory involves determining the conductivity via a time-dependent analysis which leads to $C_k \approx 5$ and provides significantly improved agreement with published data [31]. The new equation that takes into account the volume fraction and particle properties is given by

$$(20) \qquad k_{nf} = \frac{k_{bf}}{(1 - \phi^{1/3})^2}\left[(1 - \phi) + \phi\frac{\rho_{np}c_{np}}{\rho_{bf}c_{bf}}\right]\frac{n - 1}{2(n + 1)}\left[\frac{1 + \phi^{1/3}}{2} - \frac{1}{n + 1}\right]^{-1},$$

where $n = 2.233$ is a constant determined by the boundary condition [31].

To reduce the complexity of the system we now make the following assumptions:

(1) Viscous dissipation is negligible, $\Phi \approx 0$. This will be the case for most standard nanofluid flows and is clear from the numerical solutions provided in [21] for flow with $U \approx 2$m/s in a channel of around 50μm. Their results for water and CuO nanoparticles showed a negligible difference with and without viscous dissipation, while excluding the dissipation in ethylene glycol led to a very slight difference.

(2) Taking $\phi \ll 1$ we may write $f \approx \phi\rho_{np}/\rho_{bf}$. Nanofluids typically used for cooling purposes have a low volume fraction of nanoparticles.

(3) Gravity is negligible (this is simply so we may focus on the heat transfer, rather than the driving force).

(4) The system is in a steady state, so we are considering the fully-developed region.

Under these assumptions the flow is now governed by

$$\nabla \cdot (\rho_{nf}\mathbf{u}) = 0 \tag{21}$$

$$\rho_{nf}\mathbf{u} \cdot \nabla\mathbf{u} = -\nabla p + \nabla \cdot (\tilde{\tau}) \tag{22}$$

$$\nabla \cdot (\chi_{nf}\mathbf{u}T) = \nabla \cdot (k_{nf}\nabla T) \tag{23}$$

$$\nabla \cdot (\rho_{nf}\phi\mathbf{u}) = \nabla \cdot \left[C_B T \nabla\phi + C_T \phi \frac{\nabla T}{T} \right] . \tag{24}$$

In the following section we will analyse this system subject to a uniform flux condition along a flat boundary, $y = 0$,

$$k_{nf}T_y = -Q . \tag{25}$$

The flow is subject to no-slip conditions at $y = 0$

$$u = v = 0 , \tag{26}$$

while the inlet values, at $x = 0$, are defined as

$$\phi = \phi_B \qquad T = T_\infty \qquad \mathbf{u} = (U, 0). \tag{27}$$

The above system is almost identical to that of Buongiorno [5]. To obtain that system requires assuming incompressible flow (so reducing equation (21) to $\nabla \cdot \mathbf{u} = 0$), setting $C_B = D_B/T$, $C_T = D_T/\phi$ in (24) gives [5, eq. (19)], the energy equation [5, eq. (23)] differs from our equation (23) since it includes thermophoresis and Brownian motion. However, the scaling later shows this to be negligible (in [5] the Lewis number, of order 10^5, divides both terms) and in fact both terms are neglected in all subsequent analysis. Savino and Paterna [34] work in terms of mass fraction rather than ϕ. Their system is also similar to ours, but they retain the time dependence and include gravity in the momentum equation to permit buoyancy effects.

In the following section we carry out the standard boundary layer analysis on equations (21-24) to determine the fluids ability to remove heat. This requires us to augment the boundary conditions (25-27) with the far-field conditions

$$u = U \qquad v = 0 \qquad T = T_\infty \qquad \text{as} \quad y \to \infty . \tag{28}$$

4. Steady-state boundary layer analysis

The standard boundary layer scaling [1] has

$$\hat{x} = \frac{x}{L} \qquad \hat{y} = \frac{y}{L}\sqrt{Re} \qquad \hat{T} = \frac{T - T_\infty}{A} \tag{29}$$

$$\hat{u} = \frac{u}{U} \qquad \hat{v} = \frac{v}{U}\sqrt{Re} \qquad \hat{p} = \frac{p - p_\infty}{\rho_{bf}U^2}, \tag{30}$$

where U is the flow velocity in the far field (equal to the inlet velocity), $Re = \rho_{bf}UL/\mu_{bf}$ is the Reynolds number and A is an as yet undetermined temperature scale. An important point to note here is that we take U as a fixed velocity scale, that is, it does not vary with ϕ. Using scalings independent of particle load allows us to directly compare results in subsequent sections but, since an increase in ϕ will lead to an increased viscosity, this means that fixed U requires an increase in pressure gradient. In the following section we will show that the heat transfer decreases with increasing ϕ, however since U is fixed our result actually shows the HTC in a better light than it deserves. In fact, not only does the HTC decrease with increasing ϕ with our model but it also costs more energy to move the fluid.

The variable physical parameters are scaled with the base fluid value

$$(31) \qquad \hat{\mu}_{nf} = \frac{\mu_{nf}}{\mu_{bf}} \qquad \hat{\rho}_{nf} = \frac{\rho_{nf}}{\rho_{bf}} \qquad \hat{k}_{nf} = \frac{k_{nf}}{k_{bf}} \qquad \hat{\phi} = \frac{\phi}{\phi_B} \qquad \hat{\chi}_{nf} = \frac{\chi_{nf}}{\chi_{bf}}\,.$$

At present this scaling will lead to a form of boundary layer system. To simplify the problem we first examine the effect of the scaling on the ϕ equation (24). Dropping the hat notation this becomes

$$(32) \qquad \nabla \cdot (\rho_{nf}\phi\mathbf{u}) = \gamma \frac{\partial}{\partial y}\left[(T + T_\infty/A)\phi_y + \lambda\phi\frac{T_y}{T + T_\infty/A}\right]$$

where $\gamma = C_B A/\mu_{bf}$, $\lambda = C_T/(C_B A)$. The temperature scale is chosen based on the input of heat to the system, so we non-dimensionalize the boundary condition in equation (25), $\frac{KA\sqrt{Re}}{L}T_y = -Q$, and choose $A = QL/(k_{bf}\sqrt{Re})$. In Table 1 we present the device and material properties for Ethylene Glycol (EG) and water based nanofluids with Al_2O_3 particles, from which the values for the coefficients in the non-dimensional equations are calculated: these are presented in Table 2. For both EG and water $\gamma = \mathcal{O}(10^{-7}) \ll 1$ and so the right hand side of (32) is negligible. Consequently we may write

$$(33) \qquad \nabla \cdot (\rho_{nf}\phi\mathbf{u}) = \phi\nabla \cdot (\rho_{nf}\mathbf{u}) + \rho_{nf}\mathbf{u}\cdot\nabla\phi \approx 0\,.$$

The steady-state continuity equation, equation (21), allows us to reduce this to

$$(34) \qquad \mathbf{u}\cdot\nabla\phi = 0\,.$$

The physical significance of this equation is that ϕ is constant along the streamlines. From the inlet condition we know $\phi = \phi_B$ and so on all streamlines $\phi = \phi_B$ everywhere. Since $\gamma = \mathcal{O}(10^{-7})$ for water the approximation $\phi = \phi_B$ is accurate to $10^{-5}\%$, and for ethylene glycol it is even more accurate. Put another way, since the diffusion effects due to Brownian motion and thermophoresis are so small the particles simply move with the fluid and, in particular, are not affected by the heat input at the boundary. Although the value of γ may vary with the nanofluid or heat flux, its miniscule value indicates particle diffusion through Brownian motion or thermophoresis *is unlikely to ever play an important role in the boundary layer flow of a nanofluid*. This concurs with the findings of Evans *et al.* [14],

who used molecular dynamics to demonstrate that Brownian motion has only a minor effect on the enhancement of thermal conductivity of nanofluids.

The conclusion that $\phi = \phi_B$ has significant implications for the mathematical model, for example it shows that physical quantities such as ρ_{nf}, μ_{nf} and k_{nf} are also constant and determined via (10), (20) and (17,18). With constant physical quantities we may apply standard boundary layer theory to the u and T equations.

TABLE 1. Device and material properties of water and Ethylene Glycol (EG) based nanofluids with Al_2O_3 nanoparticles.

Quantity	Symbol	Units	Value
Particle diameter	d_p	m	20×10^{-9}
Far-field temperature	T_∞	K	300
Plate flux	Q	Wm^{-2}	10^7
Length of plate	L	m	10^{-2}
Far-field velocity	U	ms^{-1}	10^{-1}
Thermal conductivity (Al_2O_3, EG, H_2O)	k_{np}, k_{bf}	$Wm^{-1}K^{-1}$	30, 0.258, 0.609
Density (Al_2O_3, EG, H_2O)	ρ_{np}, ρ_{bf}	kgm^{-3}	3950, 1108.8, 10^3
Specific heat capacity (Al_2O_3, EG, H_2O)	c_{np}, c_{bf}	$Jg^{-1}K^{-1}$	800, 2360, 4187
Viscosity (EG, H_2O)	μ_{bf}	Nsm^{-2}	1.61×10^{-2}, 10^{-3}
Boltzmann's constant	k_B	JK^{-1}	1.38×10^{-23}

TABLE 2. Values of coefficients in non-dimensional equations based on properties given in Table 1.

Quantity	Ethylene Glycol	Water
C_B	4.3825×10^{-15}	7.0559×10^{-14}
C_T	3.1918×10^{-8}	5.0721×10^{-9}
β	0.0022	0.0051
Re	68.8696	10^3
Pr	147.2713	6.8752
A	4.6705×10^4	5.1926×10^3
γ	1.2714×10^{-8}	3.6638×10^{-7}
λ	155.9362	13.8437

With the above scaling the governing steady-state equations become

$$\frac{\partial u}{\partial x} + \frac{\partial v}{\partial y} = 0 \tag{35}$$

$$\rho_i \left(u \frac{\partial u}{\partial x} + v \frac{\partial u}{\partial y} \right) = -\frac{\partial p}{\partial x} + \mu_i \frac{\partial^2 u}{\partial y^2} + \mathcal{O}(1/Re) \tag{36}$$

$$0 = \frac{\partial p}{\partial y} + \mathcal{O}(1/Re) \tag{37}$$

$$u \frac{\partial T}{\partial x} + v \frac{\partial T}{\partial y} = \frac{k_i}{\chi_i} \frac{1}{Pr} \frac{\partial^2 T}{\partial y^2} + \mathcal{O}(1/Re) \,, \tag{38}$$

where the subscript i denotes the inlet value of each quantity for the nanofluid and the Prandtl number $Pr = \mu_{bf}\chi_{bf}/(\rho_{bf}k_{bf})$. Equation (37) indicates $p = p(x)$. In keeping with standard boundary layer theory we note that approaching the far-field $u \to 1$, $v \to 0$ and so equation (36) determines $p_x = 0$. Hence the problem is now described by (35) and

$$u \frac{\partial u}{\partial x} + v \frac{\partial u}{\partial y} = \nu_i \frac{\partial^2 u}{\partial y^2} \tag{39}$$

$$u \frac{\partial T}{\partial x} + v \frac{\partial T}{\partial y} = \frac{k_i}{\chi_i} \frac{1}{Pr} \frac{\partial^2 T}{\partial y^2} \,, \tag{40}$$

where $\nu_i = \mu_i/\rho_i$. These equations and the subsequent boundary conditions could be further simplified by choosing the inlet values of the physical parameters in the scaling but this would mean that the length and height scales would vary for each inlet volume fraction. Using the base fluid values means that our subsequent results may be compared on the same graph, with the same scales.

The imposed non-dimensional boundary conditions are

$$u = v = 0, \qquad k_i T_y = -1 \qquad \text{at} \qquad y = 0, \tag{41}$$

$$u = 1, v = 0, \qquad T = 0 \qquad \text{as} \qquad y \to \infty. \tag{42}$$

4.1. **Flow over a flat plate.** The well-known Blasius solution for boundary layer flow over a flat plate (see [1] for example) involves first introducing a stream function ψ where

$$u = \frac{\partial \psi}{\partial y} \qquad v = -\frac{\partial \psi}{\partial x} \,. \tag{43}$$

This automatically satisfies the continuity equation, (35). The similarity variable $\eta = y/\sqrt{2\nu_i x}$ is then introduced. To satisfy the momentum equation, (39), requires $\psi = \sqrt{2\nu_i x} f(\eta)$ where f is an unknown function determined from

$$f''' + f f'' = 0 \,, \tag{44}$$

where primes denote differentiation with η. This is simply the transformed version of equation (39). The boundary conditions $u = v = 0$ at $y = 0$ and $u \to 1$ as

$y \to \infty$ become

$$(45) \qquad f(0) = f'(0) = 0 \qquad f'(\infty) = 1 \,.$$

In fact this boundary value problem may simplified using Töpfer's transformation $f(\eta) = rF(r\eta)$, where $r > 0$ is a constant. The Blasius equation remains the same

$$(46) \qquad F''' + FF'' = 0 \,,$$

but it may be solved subject to the conditions

$$(47) \qquad F(0) = 0 \qquad F'(0) = 0 \qquad F''(0) = 1 \,,$$

that is, we solve an initial value problem (which is much easier to deal with than a boundary value problem). The solutions of the two systems will coincide provided

$$(48) \qquad f'(\infty) = r^2 F'(\infty) = 1$$

which then requires $r = (F'(\infty))^{-1/2}$. The numerical solution of (46,47) determines $r \approx 0.7773$.

The same transformation could be used to reduce the heat equation but the flux condition at $y = 0$ does not permit a similarity form. Consequently, at this stage we must look for an approximate solution form.

4.2. Solution by Heat Balance Integral Method (HBIM).

A standard approximate method to analyse boundary layer flow was developed by von Karman and Pohlhausen. From this stemmed the Heat Balance Integral Method (HBIM) which is primarily used on thermal problems. Obviously we are interested in the boundary layer flow, but there has been much more research on the HBIM so we will use techniques developed for this method to analyse the current problem. Specifically, we will employ a technique described in [29] to approximate the momentum and thermal boundary layer flow of a power law fluid.

If we consider the flow equation, equation (39), then the HBIM involves choosing a simple function to approximate the velocity over a finite boundary layer $\delta(x)$. For $y > \delta$ the deviation of velocity from that of the bulk flow is negligible (although we do not define what constitutes negligible). In this case the velocity boundary layer would be defined by the boundary conditions $u(x, \delta) = 1$ and $u_y(x, \delta) = 0$. If the approximating function is a polynomial of the form

$$(49) \qquad u = a_0 + a_1 \left(1 - \frac{y}{\delta}\right) + a_p \left(1 - \frac{y}{\delta}\right)^p \,,$$

then the conditions $u(x, \delta) = 1$ and $u_y(x, \delta) = 0$ determine $a_0 = 1, a_1 = 0$. The no-slip condition at $y = 0$ determines $a_p = -1$ and so

$$(50) \qquad u = 1 - \left(1 - \frac{y}{\delta}\right)^p \,.$$

The expression for u involves two unknowns, $\delta(x)$ and p. The velocity boundary layer thickness is determined by integrating equation (39) over the region $y \in [0, \delta]$

$$(51) \qquad \int_0^\delta uu_x + vu_y dy = \nu_i \int_0^\delta u_{yy} dy .$$

Noting from the continuity equation (35) $u_x = -v_y$, we may write the above integral momentum equation

$$(52) \qquad \frac{d}{dx} \int_0^\delta u(1 - u)dy = \nu_i \left. \frac{\partial u}{\partial y} \right|_{y=0},$$

see [8, 29] for more details. Substituting for u from equation (50) leads to a single ordinary differential equation for δ with solution

$$(53) \qquad \delta = \alpha\sqrt{x}$$

where $\alpha = \sqrt{2\nu_i(p+1)(1+2p)}$ and $\delta(0) = 0$. The standard HBIM and the von Karman-Pohlhausen technique take $p = 2$ however a more accurate method, developed by Myers [27, 28] is to choose p to minimise the least-squares error when the approximating function is substituted back into the momentum equation. In this case the error function is defined as

$$(54) \qquad E_p = \int_0^\delta \left(\frac{\partial G}{\partial x} - \nu_i \frac{\partial^2 u}{\partial y^2} \right)^2 dy$$

where $G = u(u-1)$. Note that ν_i is a function of the inlet values, and so depends on the inlet volume fraction. Consequently the optimal p value could also vary with the volume fraction, however our calculations with ϕ_B varying between 1% and 10% show $p = 2.7237$ with less than a 10^{-2}% variation. To demonstrate the result of this mehtod in Figure 1 we compare velocity profiles of (50) with $p = 2.7237$ and that of the Blasius soltuion at $x = 0.1$ with $\phi_B = 5$%. Near the surface, $y = 0$, the agreement is excellent. For $y > 1$ there is some divergence, but the solutions both end close to $y = 2.5$ (indicating the δ calculation is accurate). However, for practical purposes the important point is that the approximation works well near the boundary, so allowing an accurate calculation of the drag coefficient. The decay to the far field velocity is of less practical importance. In [29] the similarity solution for a Newtonian fluid with a fixed temperature boundary condition was also calculated and compared with the HBIM solution. Again the approximation was excellent near the boundary (in fact better than the velocity boundary layer). In this case it allowed the HTC to be accurately calculated.

For the energy equation we define δ_T as the thickness of the thermal boundary layer, then the conditions $T(x, \delta_T) = 0, T_y(x, \delta_T) = 0, k_i T_y(x, 0) = -1$ determine the temperature profile

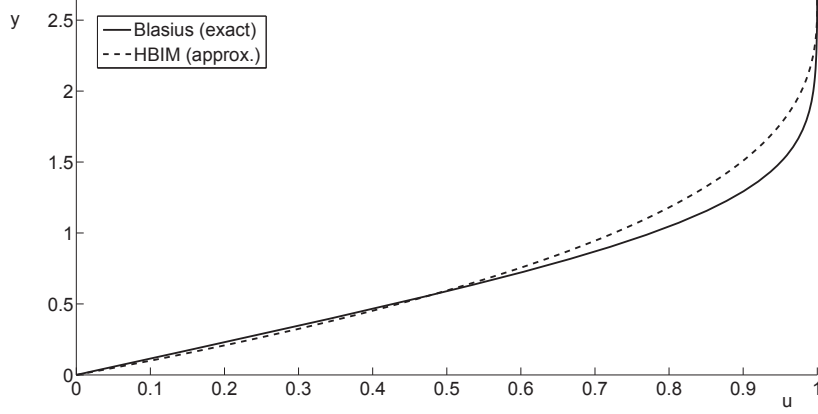$$(55) \qquad T = \frac{\delta_T}{k_i q} \left(1 - \frac{y}{\delta_T} \right)^q .$$

FIGURE 1. Comparison of the exact Blasius and approximate HBIM solutions for the velocity profile at $x = 0.1$ with $\phi_B = 5\%$.

The heat balance integral is determined by integrating the energy equation (40) over $y \in [0, \delta_T]$

$$(56) \qquad \frac{d}{dx}\int_0^{\delta_T} uT dy = -m_i \left.\frac{\partial T}{\partial y}\right|_{y=0} = \frac{m_i}{k_i}$$

where $m_i = k_i/(\chi_i Pr)$, see [29] for details.

Substituting for u, T from (50,55) requires numerical integration since p is a non-integer, however an analytical solution is preferred so, following [8, 29], we assume that the thermal boundary layer is much smaller than the velocity boundary layer

$$(57) \qquad \delta_T = \epsilon\delta$$

where $\epsilon \ll 1$ (this is confirmed *a priori*) is to be determined. On applying this to (50) and noting that within the HBI $y \ll \delta_T$ we can make the approximation

$$(58) \qquad u \approx 1 - \left(1 - \frac{py}{\delta}\right) = \frac{py}{\delta}.$$

Now the HBI (56) may be integrated analytically giving

$$(59) \qquad \epsilon = \sqrt[3]{\frac{m_i q(q+2)(q+1)}{p\alpha^2}}.$$

For $\phi_b \in [1, 10]\%$ the value of the small parameter varies $\epsilon \in [0.2971, 0.2635]$. The exponent q is found by minimising the error

$$(60) \qquad E_q = \int_0^{\delta_T} \left(\frac{\partial F}{\partial x} - m_i\frac{\partial^2 T}{\partial y^2}\right)^2 dy$$

where $F = uT$. According to equation (60) the value of q may vary with m_i, which depends on k_i, χ_i and Pr, so it may be a function of material properties and volume fraction. For water, with $\phi_B \in [1, 10]\%$ we find $q = 1.9975$ (with less than 0.01% variation), for EG $q = 2.014$ (with less than 0.4% variation).

With no analytical solution to verify the thermal approximation we developed a finite difference code to solve equations (35,39,40) subject to boundary conditions (41,42) and inlet conditions $u = 1, v = 0$ and $T = 0$. The semi-infinite y range was cut off at large y where conditions (42) applied. For example at $x = 0.1$ it was sufficient to calculate results to $y = 5$. Standard finite difference approximations were made for the derivatives in y and the solution was marched in x with implicit stepping. The results showed reasonable agreement with the temperature profiles predicted by equation (55) with the worst disagreement occurring at $y = 0$. With $x = 0.1$ the HBIM and numerical solutions differed by approximately 10%. We will discuss this difference later with regard to Figure 4.
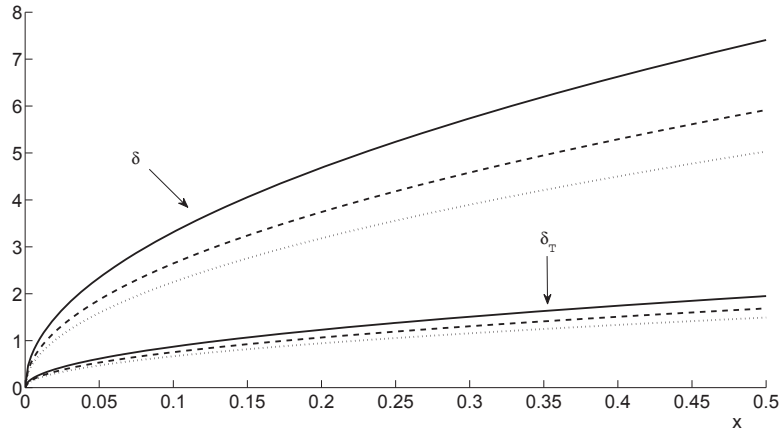

FIGURE 2. Delta profiles are compared for different volume fractions; $\phi_B = 1, 5, 10\%$ are represented by dotted, dashed and solid lines, respectively, for a Al_2O_3-water nanofluid.

In Figure 2 we plot velocity and thermal boundary layers for three different volume fractions, $\phi_B = 1, 5, 10\%$ which are represented by dotted, dashed and solid lines respectively. First we note that $\delta_T \ll \delta$ in all cases, confirming the assumption made earlier. A more important point is that the thermal boundary layer thickness increases with volume fraction suggesting that the nanofluid could indeed extract more heat with higher nanoparticle concentrations. In Figure 3 we show the velocity profile $u(y)$ at $x = 0.05$ for the same three volume fractions. Here we note that velocity decreases with increasing volume fraction, indicating that the mass transport is slower, which may then have an adverse effect on heat transport.
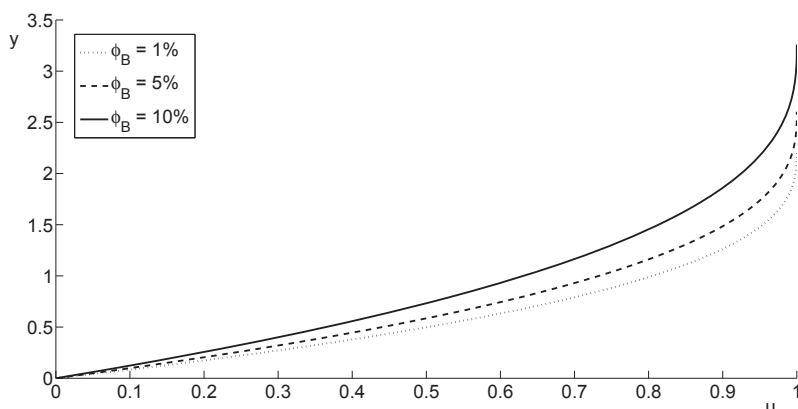
FIGURE 3. Velocity profiles predicted by the HBIM for different volume fractions: $\phi_B = 1, 5, 10\%$ are represented by dotted, dashed and solid lines, respectively, for a Al_2O_3-water nanofluid.

Figures 2 and 3 show the trade off between increasing the heat flow (through increasing k) whilst decreasing the fluid flow (through increasing μ) by adding nanoparticles. To determine which effect is dominant we now return to the HTC calculation. Defining a non-dimensional HTC $\hat{h} = Lh/(k_{bf}\sqrt{Re})$ and dropping the hat notation, equation (5) may be written

$$(61) \qquad h_{nf} = \frac{\int_0^{\delta_T} u \, dy}{\int_0^{\delta_T} uT \, dy} \ .$$

In Figure 4 the HTC (61) is plotted against the device length for three values of the volume fraction, $\phi_B = 1, 5, 10\%$, and the base fluid. What is clear from this graph is that the HTC decreases with increasing volume fraction. Furthermore, as discussed earlier the velocity scale U is fixed in all cases, and so an increase in ϕ_B (which increases viscosity) requires an increase in Δp. So with higher particle loadings the system requires more energy to move the fluid and this further decreases the system's efficiency. That is, according to the present mathematical model and for the cases we have studied for fluid and heat flow of a nanofluid there is *no augmentation in the HTC*; in fact it appears that the opposite occurs, despite the numerous claims based on the same theory. However, our theoretical result does concur with Ding *et al.* [12] who state that nanofluids with an enhanced thermal conductivity do not guarantee an enhancement in the convective heat transfer. Earlier we discussed the error in using the HBIM approximation to the temperature. At $x = 0.1$ we found an error of approximately 10% between the approximate and numerical solutions. From Figure 4 we see that there is an approximately 30% decrease in HTC, which cannot be explained away by a 10% error in temperature. In the following section we will discuss why so many

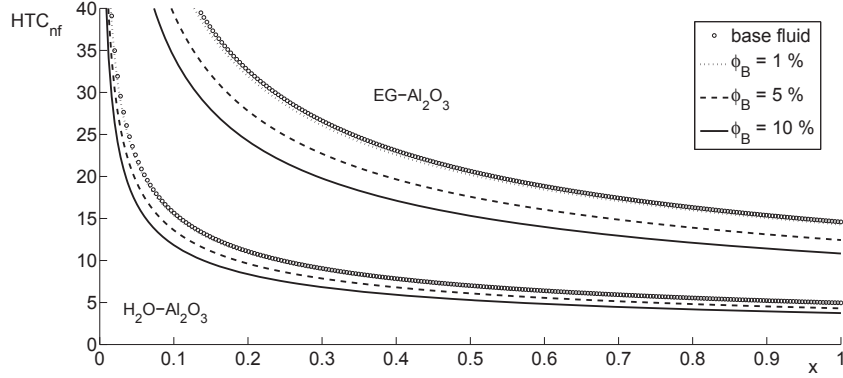researchers have found the opposite result to ours using a similar initial set of equations.

FIGURE 4. Variation of the heat transfer coefficient along the surface for the base fluid (Ethylene glycol or water) and $\phi_B = 1, 5, 10\%$

5. APPARENT IMPROVEMENT IN HTC?

Buongiorno [5] wrote the seminal paper describing the mathematical model for nanofluid heat transfer including thermophoresis and Brownian motion. Savino and Patterson [34] developed a similar model accounting for gravity effects. Numerous theoretical studies have been based on the form of model developed in these two papers and, in contrast to the present conclusion, the authors generally conclude that the HTC increases with volume fraction. This raises the obvious question of why do our results differ from this previous body of work? There exist too many studies to go through each one individually, so now we will focus on a few highly cited ones.

Buongiorno's model is a special case of that described in the present paper. In §5 of his paper he investigates the HTC in a 'laminar sublayer' where the flow is described by

$$(62)\frac{\partial}{\partial y}\left(\mu_{nf}\frac{\partial v}{\partial y}\right) = 0 \quad \frac{\partial}{\partial y}\left(k_{nf}\frac{\partial T}{\partial y}\right) = 0 \quad \frac{\partial}{\partial y}\left(D_B\frac{\partial \phi}{\partial y} + \frac{D_T}{T}\frac{\partial T}{\partial y}\right) = 0\,.$$

This region is matched to a turbulent sublayer. Equations (62) are formally derived from equations (22-24) by rescaling height to focus on a region close to the wall. To reproduce this we alter the scaling given by equations (29,30) to $y = H\bar{y}, v = HU\bar{v}/L$, where H is an as yet unspecified height-scale (previously

we chose $H = L/\sqrt{Re}$). Scaling equation (24) leads to

$$(63) \qquad \nabla \cdot (\rho_{nf}\phi\mathbf{u}) \;\; = \;\; \frac{C_B A L}{H^2 \rho_{bf} U} \frac{\partial}{\partial y} \left[(T + T_\infty/A)\phi_y + \lambda\phi \frac{T_y}{T + T_\infty/A} \right] .$$

In the analysis of the previous sections we neglected the right hand side of this equation since the leading coefficient was small, now to retrieve the third equation in (62) we require this same coefficient to be large which indicates

$$(64) \qquad H^2 \ll \frac{C_B A L}{\rho_{bf} U} \quad \Rightarrow \quad H \ll \frac{C_B q L}{\rho_{bf} k_{bf} U},$$

after applying the definition $A = qH/k_{bf}$. To get some idea of the thickness H of this sublayer consider water flowing at a velocity 1cm/s over a section with $L = 1\text{cm}$ and $C_B = 7 \times 10^{-14}$, as shown in Tables 1 and 2. This results in $H \ll 1\text{nm}$. Travis $et\ al.$ [35], compared molecular dynamics simulations to computations based on the Navier-Stokes equations, to show that continuum theory may only be applied to water flow down to around 3nm. A further issue is that it is well known from experiments that the actual laminar sublayer has a thickness $\delta \approx 11.6\mu/(\rho U)$, taking the base fluid values for the viscosity and density from Table 1 gives $\delta \approx 1.2\text{mm}$. So, with water as the base fluid the system of equations (62) apply in a region around 6 orders of magnitude thinner than the actual laminar sublayer and so cannot be matched to the outer turbulent region, also they are valid on a height-scale much smaller than that required by the continuum limit.

Our analysis in the previous section used boundary layer theory. This is a standard technique to determine flow and heat transfer at a boundary. The key to boundary layer theory is finding an appropriate similarity variable which transforms the governing partial differential equations to ordinary differential form. Kuznetsov and Nield [23] add buoyancy to Buongiorno's system and seek similarity solutions involving the variable $\eta \propto y/x^{1/4}$. Their governing equation for ϕ then reduces to an ordinary differential equation,

$$(65) \qquad g'' + \frac{3}{4} L_e \psi g' + \frac{N_t}{N_b} \theta'' = 0$$

where g, θ are the functions representing the non-dimensional ϕ, T and ψ is the stream function. The strength of Brownian motion and thermophoresis are represented by the coefficients N_b, N_t respectively and $L_e = \alpha_{nf}/D_B$ is the Lewis number. Values for these coefficients are calculated in [5] (with N_b/N_t denoted N_{BT}). The values quoted for water containing 10nm alumina nanoparticles are $L_e = 8 \times 10^5, N_{BT} = 0.2$; for 10nm copper nanoparticles $L_e = 7 \times 10^5, N_{BT} = 2$. The extremely high value of Le indicates that the non-dimensional equation (65) is incorrectly scaled. Dividing through by L_e leads to $g' \approx 0$ and consequently ϕ is constant (as determined in our analysis). However, the results presented in [23] show a significant variation in g, which then affects the velocity and temperature

profiles (since g appears in all three governing equations) and consequently the heat transfer. The reason for this difference between our conclusion of constant ϕ and theirs is that they choose $L_e = 10$, rather than the correct physical value. The larger value would make the boundary layer thickness negligible. However, the negligible terms in (65) could be retained by introducing a new height scale (of the order $1/L_e$ smaller than the boundary layer height-scale) but again this brings us to the limit of continuum theory.

Khan and Pop [18] use a slightly different scaling to [23] for the similarity variable to obtain an equation almost identical to (65). Their Lewis number is defined as $L_e = \nu/D_B$, where ν is the kinematic viscosity. For water $\nu \approx 10^-6$ and so $L_e \in [10^4, 10^6]$. They also employ the value $L_e = 10$.

Savino and Paterna [34] study a system almost identical to our initial system (6–9). The focus of their study is convective motion of a nanofluid contained between two differentially heated plates held 1mm apart and they do determine a difference in motion due to the effects of thermophoresis and Brownian motion. However, their time-scale is of the order 10^5s or 27 hours for motion in a 1mm gap and the results are most noticeable in conditions where gravity is 10^{-6} of the standard value.

6. CONCLUSION

In this paper we have developed a model for nanofluid flow including the effects of thermophoresis and Brownian motion with the aim of determining whether nanofluids improve heat removal. The heat transfer coefficient was examined within standard boundary layer theory. The boundary layer formulation showed quite clearly that, close to the substrate thermophoresis and Brownian motion effects are negligible compared to advection. Consequently the particle volume fraction remains constant along the streamlines and so the fluid properties, such as density, viscosity and specific heat, are also constant.

The most significant result of this analysis is the clear decrease in the heat transfer coefficient as the particle concentration increases. Our results were somewhat flattering with regards to the HTC since we used a fixed far-field velocity. This means that as the particle concentration increases, and so the viscosity also increases, the pressure drop or pumping power must also be increased. So, not only did the HTC decrease with particle concentration but it cost more energy to pump the fluid.

Our result contradicts many analyses based on similar governing equations, however, it is backed up by recent experimental evidence, see [6, 12] for example. Our model also required a number of assumptions and simplifications, but these could all be quantified and are not of sufficient magnitude to alter our conclusion regarding the heat transfer. Possible reasons for this discrepancy between our conclusion and that of previous papers include the rather loose definition of

heat transfer coefficient prevalent in the literature and a number of unjustified assumptions and approximations as well as incorrect parameter values.

This paper does not prove that nanofluids cannot improve heat removal. It may be that the enhancement observed in some experiments is due to a physical effect not included in our model. Further, we have only presented results for water or ethylene glycol based fluids with Al_2O_3 particles (although results with CuO particles were found to be similar) in a single flow configuration. It is possible that some other fluid-solid combinations may have a beneficial effect on heat transfer. However, given the clear deterioration in HTC shown by our calculations, there would need to be a marked change in the fluid properties (such as a much larger increase in thermal conductivity coupled with a significantly lower viscosity increase) for the current form of model to suggest nanofluids improve heat removal capacity.

Acknowledgements

References

[1] Acheson DJ (1990) Elementary Fluid Dynamics. Oxford University Press.
[2] Astumian RD Coupled transport at the nanoscale: The unreasonable effectiveness of equilibrium theory. Proc. Nat. Acad. Sci. 104(1):3–4.
[3] Bejan A (2004) Convection Heat Transfer (3rd Ed.) John Wiley and Sons.
[4] Bird R, Stewart W, Lightfoot E (2007) Transport phenomena. John Wiley & Sons.
[5] Buongiorno J (2006) Convective Transport in Nanofluids. Journal of Heat Transfer 128:240–250.
[6] Buongiorno J, Venerus D, Prabhat N, McKrell T, Townsend J et al(2009) A benchmark study on the thermal conductivity of nanofluids. Journal of Applied Physics 106, 094312.
[7] Brenner H, Bielenberg JR (2005) A continuum approach to phoretic motions: Thermophoresis. Physica A 355:251–273.
[8] Chhabra RP, Richardson JF (2008) Non-Newtonian flow and applied rheology (2nd Ed.) Butterworth-Heinemann.
[9] Corcione M (2011) Empirical correlating equations for predicting the effective thermal conductivity and dynamic viscosity of nanofluids. Energy Conversion and Management 52:789–793.
[10] Das S, Putra N, Thiesen P, Roetzel W (2003) Temperature Dependence of Thermal Conductivity Enhancement for Nanofluids. J. Heat Transfer 125:567–574.
[11] Daungthongsuk W, Wongwises S (2007) A critical review of convective heat transfer of nanofluids. Renewable and Sustainable Energy Reviews 11:797–817

[12] Ding Y, Chen H, He Y, LapkinA, Yeganeh A, Siller L and Butenko YV (2007) Forced convective heat transfer of nanofluids. Advanced Powder Technol. 18:813–824.

[13] Duhr S, Braun D (2006) Why molecules move along a temperature gradient. Proc. Nat. Acad. Sci. 103(52): 19678–19682.

[14] Evans W, Fish J, Keblinski P (2006) Role of Brownian motion hydrodynamics on nanofluid thermal conductivity. Applied Physics Letters 88, 093116.

[15] Haddad Z, Abu-Nada E, Oztop HF, Mataoui A (2012) Natural convection in nanofluids: Are the thermophoresis and Brownian motion effects significant in nanofluid heat transfer enhancement? International Journal of Thermal Sciences 57:152–162.

[16] Hwang KS, Jang SP, Choi SUS (2009) Flow and convective heat transfer characteristics of water-based Al2O3 nanofluids in fully developed laminar flow regime. International Journal of Heat and Mass Transfer 52:193–199.

[17] Jang SP, Choi SUS (2006) Cooling performance of a microchannel heat sink with nanofluids. Applied Thermal Engineering 26(17–18):2457–2463.

[18] Khan WA, Pop I (2010) Boundary-layer flow of a nanofluid past a stretching sheet. Int. J. Heat Mass Trans. 53:2477–2483 doi:10.1016/j.ijheatmasstransfer.2010.01.032

[19] Khanafer K., Vafai K. A critical synthesis of thermophysical characteristics of nanofluids. International Journal of Heat and Mass Transfer 54 (2011) 4410–4428. doi:10.1016/j.ijheatmasstransfer.2011.04.048

[20] Kleinstreuer C, Feng Y Experimental and theoretical studies of nanofluid thermal conductivity enhancement: a review. Nanoscale Research Letters 2011, 6:229 http://www.nanoscalereslett.com/content/6/1/229

[21] Koo J, Kleinstreuer C (2005) Laminar nanofluid flow in microheat-sinks. International Journal of Heat and Mass Transfer 48:2652–2661.

[22] Kuznetsov AV, Nield DA (2010) Natural convective boundary-layer flow of a nanofluid past a vertical plate. International Journal of Thermal Sciences 49(2):243–247.

[23] Kuznetsov AV, Nield DA (2010) Natural convective boundary-layer flow of a nanofluid past a vertical plate International Journal of Thermal Sciences 49:243–247.

[24] Lee J, Mudawar I (2007) Assessment of the effectiveness of nanofluids for single-phase and two-phase heat transfer in micro-channels. International Journal of Heat and Mass Transfer 50(3–4):452–463.

[25] Maiga SEB, Nguyen CT, Galanis N, Roy G (2004) Heat transfer behaviors of nanofluids in a uniformly heated tube. Superlatt. Microstruct. 35:543–557.

[26] McNab GS, Meisen A (1973) Thermophoresis in Liquids. J. Colloid Interface Sci. 44(2).

[27] Myers TG (2009) Optimizing the exponent in the heat balance and refined integral methods, Int. Commun. Heat Mass Transfer 36(2):143–147.

[28] Myers TG (2010) Optimal exponent heat balance and refined integral methods applied to Stefan problems, Int. J. Heat Mass Transfer 53:1119–1127.

[29] Myers TG (2010) An approximate solution method for boundary layer flow of a power law fluid over a flat plate. International Journal of Heat and Mass Transfer 53: 2337–2346. doi:10.1016/j.ijheatmasstransfer.2010.02.006

[30] Myers TG, Mitchell SL and Font F (2012) Energy conservation in the one-phase supercooled Stefan problem, Int. Commun. Heat Mass Trans. 39, 1522–1525. http://dx.doi.org/10.1016/j.icheatmasstransfer.2012.09.005

[31] Myers TG, MacDevette MM, Ribera H (2013) A time dependent model to determine the thermal conductivity of a nanofluid. Journal of Nanoparticle Research 15:1775.

[32] Popa C, Polidori G, Arfaoui A, Fohanno S (2011) Heat and Mass Transfer in External Boundary Layer Flows Using Nanofluids. Heat and Mass Transfer - Modeling and Simulation. doi:10.5772/1431.

[33] Prasher R, Bhattacharya P, Phelan PE (2006) Brownian-Motion-Based Convective-Conductive Model or the Effective Thermal Conductivity of Nanofluids. Journal of Heat Transfer 128:588–595.

[34] Savino R, Paterna D (2008) Thermodiffusion in nanofluids under different gravity conditions. Physics of Fluids 20, 017101.

[35] Travis KP, Todd BD, Evans DJ (1997) Departure from Navier-Stokes hydrodynamics in confined liquids. Physical Review E 55(4).

[36] Vigolo D, Rusconi R, Stone HA, Piazza R (2010) Thermophoresis: microfluidics characterization and separation. Soft Matter 6:3489–3493.

[37] Wang X, Xu X, Choi SUS (1999) Thermal conductivity of nanoparticle-fluid mixture. J. Thermophys. Heat Transfer 13:474–480.

[38] Xuan Y, Li Q (2000) Heat transfer enhancement of nanofluids. International Journal of Heat and Fluid Flow 21(1):58–64.

[39] Xuan Y, Roetzel W (2000) Conceptions for heat transfer correlation of nanofluids. International Journal of Heat and Mass Transfer 43(19):3701–3707.

[40] Yang Y, Zhong ZG, Grulke EA, Anderson WB, Wu G (2005) Heat transfer properties of nanoparticle-in-fluid dispersion (nanofluids) in laminar flow. International Journal of Heat and Mass Transfer 48:1107–1116.

M.M. MacDevette
Centre de Recerca Matemàtica
Campus de Bellaterra, Edifici C
08193 Bellaterra
Barcelona, Spain
and
Departament de Matemàtica Aplicada I
Universitat Politècnica de Catalunya
Barcelona, Spain
    E-mail address: mmacdevette@crm.cat

T.G. Myers (corresponding author)
Centre de Recerca Matemàtica
Campus de Bellaterra, Edifici C
08193 Bellaterra
Barcelona, Spain
    E-mail address: tmyers@crm.cat

B. Wetton
Mathematics Department
University of British Columbia
Vancouver BC, Canada V6T 1Z2
    E-mail address: wetton@math.ubc.ca